# Conical diffraction of linearly polarised light controls the angular position of a microscopic object

**D. P. O'Dwyer,[1] C. F. Phelan,[1] K. E. Ballantine,[1] Y. P. Rakovich,[1] J. G. Lunney[1] and J. F. Donegan[1,2]***

[1]*School of Physics, Trinity College Dublin, Dublin 2, Ireland*
[2]*Principal Investigator, CRANN Research Institute, Trinity College Dublin, Dublin 2, Ireland*
**jdonegan@tcd.ie*

**Abstract:** Conical diffraction of linearly polarised light in a biaxial crystal produces a beam with a crescent-shaped intensity profile. Rotation of the plane of polarisation produces the unique effect of spatially moving the crescent-shaped beam around a ring. We use this effect to trap microspheres and white blood cells and to position them at any angular position on the ring. Continuous motion around the circle is also demonstrated. This crescent beam does not require an interferometeric arrangement to form it, nor does it carry optical angular momentum. The ability to spatially locate a beam and an associated trapped object simply by varying the polarisation of light suggests that this optical process should find application in the manipulation and actuation of micro- and nano-scale physical and biological objects.



**OCIS codes:** (140.7010) Laser trapping; (050.1940) Diffraction; (260.1440) Crystal optics.

## References and Links

1. C. F. Phelan, D. P. O'Dwyer, Y. P. Rakovich, J. F. Donegan, and J. G. Lunney, "Conical diffraction and Bessel beam formation with a high optical quality biaxial crystal," Opt. Express **17**(15), 12891–12899 (2009).
2. M. V. Berry, M. R. Jeffrey, and J. G. Lunney, "Conical diffraction: observations and theory," Proc. R. Soc. A. **462**(2070), 1629–1642 (2006).
3. W. R. Hamilton, "Third supplement to an essay on the theory of system of rays," Trans. R. Irish Acad. **17**, 1–144 (1837).
4. H. Lloyd, "On the phenomena presented by light in its passage along the axes of biaxial crystals," Philos. Mag. **1**, 112–120 (1833).
5. A. Ashkin, J. M. Dziedzic, J. E. Bjorkholm, and S. Chu, "Observation of a single-beam gradient force optical trap for dielectric particles," Opt. Lett. **11**(5), 288–290 (1986).
6. A. Ashkin, J. M. Dziedzic, and T. Yamane, "Optical trapping and manipulation of single cells using infrared laser beams," Nature **330**(6150), 769–771 (1987).
7. K. Svoboda, P. P. Mitra, and S. M. Block, "Fluctuation analysis of motor protein movement and single enzyme kinetics," Proc. Natl. Acad. Sci. U.S.A. **91**(25), 11782–11786 (1994).
8. C. Bustamante, S. B. Smith, J. Liphardt, and D. Smith, "Single-molecule studies of DNA mechanics," Curr. Opin. Struct. Biol. **10**(3), 279–285 (2000).
9. S. Husale, W. Grange, M. Karle, S. Bürgi, and M. Hegner, "Interaction of cationic surfactants with DNA: a single-molecule study," Nucleic Acids Res. **36**(5), 1443–1449 (2008).
10. M. Dao, C. T. Lim, and S. Suresh, "Mechanics of the human red blood cell deformed by optical tweezers," J. Mech. Phys. Solids **51**(11-12), 2259–2280 (2003).
11. M. Salomo, U. F. Keyser, M. Struhalla, and F. Kremer, "Optical tweezers to study single protein A/immunoglobulin G interactions at varying conditions," Eur. Biophys. J. **37**(6), 927–934 (2008).
12. J. E. Curtis, B. A. Koss, and D. G. Grier, "Dynamic holographic optical tweezers," Opt. Commun. **207**(1-6), 169–175 (2002).
13. P. T. Korda, M. B. Taylor, and D. G. Grier, "Kinetically locked-in colloidal transport in an array of optical tweezers," Phys. Rev. Lett. **89**(12), 128301 (2002).
14. S. B. Smith, Y. J. Cui, and C. Bustamante, "Overstretching B-DNA: the elastic response of individual double-stranded and single-stranded DNA molecules," Science **271**(5250), 795–799 (1996).

#136055 - $15.00 USD Received 4 Oct 2010; revised 12 Nov 2010; accepted 13 Nov 2010; published 13 Dec 2010

15. E. McLeod, and C. B. Arnold, "Subwavelength direct-write nanopatterning using optically trapped microspheres," Nat. Nanotechnol. **3**(7), 413–417 (2008).
16. A. Terray, J. Oakey, and D. W. M. Marr, "Fabrication of linear colloidal structures for microfluidic applications," Appl. Phys. Lett. **81**(9), 1555–1557 (2002).
17. L. Allen, M. J. Padgett, and M. Babiker, "The orbital angular momentum of light," Prog. Opt. **39**, 291–372 (1999).
18. A. T. O'Neil, I. MacVicar, L. Allen, and M. J. Padgett, "Intrinsic and extrinsic nature of the orbital angular momentum of a light beam," Phys. Rev. Lett. **88**(5), 053601 (2002).
19. J. E. Curtis, and D. G. Grier, "Structure of optical vortices," Phys. Rev. Lett. **90**(13), 133901 (2003).
20. K. Ladavac, and D. G. Grier, "Colloidal hydrodynamic coupling in concentric optical vortices," Europhys. Lett. **70**(4), 548–554 (2005).
21. L. Paterson, M. P. MacDonald, J. Arlt, W. Sibbett, P. E. Bryant, and K. Dholakia, "Controlled rotation of optically trapped microscopic particles," Science **292**(5518), 912–914 (2001).
22. D. M. Villeneuve, S. A. Aseyev, P. Dietrich, M. Spanner, M. Y. Ivanov, and P. B. Corkum, "Forced molecular rotation in an optical centrifuge," Phys. Rev. Lett. **85**(3), 542–545 (2000).
23. D. G. Grier, "A revolution in optical manipulation," Nature **424**(6950), 810–816 (2003).
24. S. Maruo, A. Takaura, and Y. Saito, "Optically driven micropump with a twin spiral microrotor," Opt. Express **17**(21), 18525–18532 (2009).
25. L. Stars, and P. Bartlett, "Colliodal dynamics in polymer solutions," Faraday Discuss. **123**, 323–334 (2002).
26. H. Sosa-Martínez, and J. C. Gutierrez-Vega, "Optical Forces on a Mie Spheroidal Particle Arbitrarily Oriented in a Counter-Propagating Trap," J. Opt. Soc. Am. B **26**(11), 2109–2116 (2009).
27. E. Sidick, S. D. Collins, and A. Knoesen, "Trapping forces in a multiple-beam fiber-optic trap," Appl. Opt. **36**(25), 6423–6433 (1997).

## 1. Introduction

It is relatively straightforward to uniformly change the intensity of a light beam; for example, for linearly polarised light, by rotating a half wave-plate in front of a linear polariser. To change the transverse intensity distribution, or reposition elements of the beam, requires more elaborate optical techniques. In this study we show that the positioning of a light beam on a circle can now be achieved in a straightforward way by combining internal conical diffraction of linearly polarised light with rotation of a half wave-plate. We also show the use of this novel beam in a new type of optical trap.

In the classic manifestation of internal conical diffraction a circularly polarised Gaussian beam is focussed into a biaxial crystal and directed along an optic axis; the beam spreads out as a cone inside the crystal and emerges as a ring-shaped beam [1]. The ring is most sharply defined at the position known as the focal image plane (FIP), which corresponds to the position of the image in the crystal of the waist of the focused Gaussian beam [2]. The ring-shaped beam has an unusual distribution of polarisation. At each point on the ring the polarisation is linear, but the plane of polarisation varies around the ring such that at diametrically opposite points the linear polarisations are orthogonal. For our studies we use linearly polarised input beam; the output beam is now crescent-shaped with a $\cos^2(\theta/2)$ intensity dependence around the ring, where $\theta$ is the azimuthal angle measured from the plane of polarisation of the input beam. Thus, a dark region lies opposite the region where the intensity is a maximum. Despite being an exemplary historical case of theoretical prediction followed by experimental verification, the discovery of conical diffraction in the 1830s at Trinity College Dublin [3, 4] has found little application in succeeding centuries.

The use of lasers to optically trap micro- and nano-scale objects is now a well established technique in Physics, Chemistry and Biology. The seminal work of Ashkin and associates in 1986 [5] has led to over 20 years of research in which many optical trapping techniques were used to manipulate microscopic objects. In the standard technique, an optical trap is formed using a tightly focused Gaussian laser beam in an optical microscope with high numerical aperture. Near the focal position there is a strong gradient force which pushes the particle towards the highest intensity region. Various trap arrangements have been studied, particularly in biology [6–11]. A holographic element, such as a spatial light modulator, can form multiple traps with from a single beam [12–14]. Optical traps have also been used as the basis for nanofabrication and as optical actuators [15, 16].

#136055 - $15.00 USD Received 4 Oct 2010; revised 12 Nov 2010; accepted 13 Nov 2010; published 13 Dec 2010

Within the last decade, there have been several demonstrations of the circular motion and rotation of small objects in an optical trap. Several groups, including those of Padgett and Grier, have shown optical beams carrying orbital angular momentum can drive rotation of microscale objects in a controlled way [17–20]. Light beams carrying orbital angular momentum are distinctly different from the commonly used Gaussian beam in that the beam has a vortex structure with zero intensity on axis. For example, the Laguerre-Gaussian (LG) beam has a ring-shaped intensity profile and carries orbital angular momentum of $\ell\,\hbar$ per photon, where $2\pi\,\ell$ is the azimuthal phase change around the beam axis. Beams with $\ell$ values up to 60 have been created and used to rotate objects [19]. The rotation arises when absorption of some of the light leads to the transfer of angular momentum from the beam to the object. Thus rotation in this type of trap depends on the optical properties of the trapped object. In 2001, the group of K. Dholakia showed that controlled rotation could be obtained using spatially structured light beam generated by optical interference [21]. There an LG beam, with $\ell$ = 2 or 3, was interfered with a Gaussian beam to produce a beam with 2 or 3 lobes. Adjustment of the relative optical phase of the LG and the Gaussian beams leads to azimuthal rotation of the lobed intensity profile. An object trapped in one of the lobes is dragged along and thus circulates around the beam axis. A clear advantage of this scheme over approaches requiring the transfer of orbital angular momentum, is that absorption of the light is not required. The ability to rotate an object about its centre of gravity, or to position it at any angle on the circumference of a circle, could be of use in optically driven machines such as a micro-centrifuge [22], or an optical actuator [23–25].

## 2. Conical diffraction of light

A narrow beam of circularly-polarised light incident along an optic axis of a biaxial crystal is transformed into a hollow, slant cone of light within the crystal and a hollow cylinder of light upon exiting the crystal. This phenomenon is known as internal conical refraction. The description of conical refraction of a finite-sized beam, which contains an angular distribution of k-vectors, requires a wave optics approach. The phenomenon is then termed conical diffraction. The paraxial approximation has been used to calculate conical diffraction of a Gaussian beam and good agreement between experiment and calculation was obtained [1,2]. When the Gaussian beam is focussed to a beam waist $w_0$, the double ring of light (radius $R_0$) is most sharply defined at the plane corresponding to the image of the beam waist in the crystal, termed the focal image plane (FIP), as indicated in Fig. 1. The FIP lies beyond the focal point of the lens at a distance determined by refraction in the crystal. Depending on the focal length and positioning of the focusing lens, the FIP may lie inside or outside the crystal. In either case, the intensity distribution in the FIP may be relayed to another position using an imaging lens [1]. The ratio of $R_0$ to $w_0$ of determines the radial intensity profile.

## 3. Conical diffraction of linearly polarised light

Light from a frequency-doubled Nd-YAG CW laser at 532 nm is focused using a converging lens ($L_1$) with focal length $f_1$ = 10 cm to a beam waist with $1/e^2$ radius of 37 μm as shown in Fig. 2. A 3 cm long slab of $KGd(WO_4)_2$, supplied by CROptics©, is used for conical diffraction. This biaxial crystal has refractive indices $n_1$ = 2.031, $n_2$ = 2.063 and $n_3$ = 2.118 at 532 nm. The crystal is placed between the lens $L_1$ and the beam waist and it is oriented such that the light propagates along one of the optic axes, which is perpendicular to the slab faces. With circularly-polarised input this arrangement generates a ring-shaped beam in the FIP with radius $R_0 = LA$ = 0.61 mm, where $L$ is the length of the crystal and A = 0.0203 radians is the semi cone angle of the light as it spreads in the crystal. The FIP lies at $f_1 + L(1-1/n_2)$ = 11.54 cm from $L_1$. A second converging lens ($L_2$) with $f_2$ = 22 cm is placed at

#136055 - $15.00 USD Received 4 Oct 2010; revised 12 Nov 2010; accepted 13 Nov 2010; published 13 Dec 2010

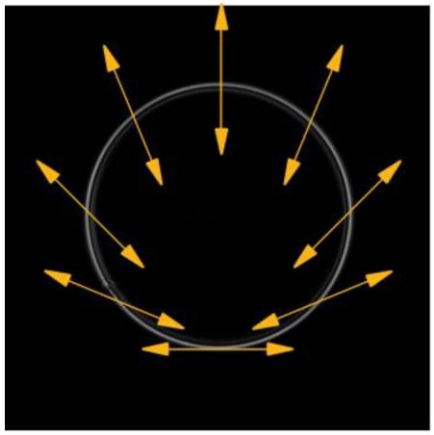

Fig. 1. Conical diffraction of circularly polarised light in the focal image plane and the polarisation distribution around the ring. The ring diameter is 0.61 mm.

22 cm from the FIP to collimate the light from each point in the FIP and thus ensure that the demagnifed image of the FIP is formed in the focal plane of the microscope objective. The diameter ($D_t$) of the ring shaped beam in the focal plane of the objective is given by:

$$D_t = 2\frac{f_3 R_0}{f_2} \tag{1}$$

The objective, $L_3$, is a Leitz NeoPlan Fluotar x100 0.9 NA infinity corrected objective with a focal length $f_3$ of 1.81 mm, giving $D_t$ = 10 μm. The power in the trapping plane is determined by replacing the sample holder with an optical power meter.

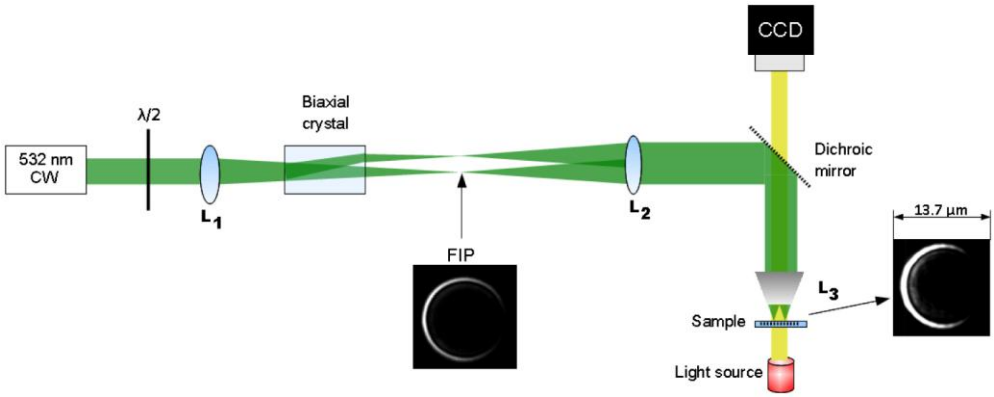


Fig. 2. Experimental set-up showing the 532 nm 200 mW laser together with a half wave-plate and a 532 nm dichroic mirror to direct the laser onto the sample and exclude it from the CCD.

A crescent-shaped beam is formed by introducing a linearly polarised beam into the biaxial crystal. The plane of polarisation of the light incident on the biaxial crystal is rotated by adjusting the angle α which the fast axis of the half wave-plate makes with the plane of polarisation of the laser. As the half wave-plate is rotated through α, the angular position of the maximum intensity is rotated through 4α. Figure 3 shows the intensity profiles at the FIP at 11.54 cm beyond $L_1$ for conical diffraction of a linearly polarised Gaussian beam as the wave-plate is rotated by 90° in $10^0$ increments. Media 1 shows the crescent beam rotating around the circle as the half wave-plate is rotated with a motorized stage.

#136055 - $15.00 USD Received 4 Oct 2010; revised 12 Nov 2010; accepted 13 Nov 2010; published 13 Dec 2010

## 4. Optical trapping using conical diffraction of linearly polarised light

To further demonstrate the unique polarisation-controlled positioning of the intensity around the ring, we use this beam to trap, circulate and rotate polystyrene and melamine-formaldehyde microspheres suspended in Millipore-filtered water. Polystyrene particles with 5.2 μm diameter and refractive index 1.55, and melamine formaldehyde particles with 5.2 μm diameter and a refractive index 1.68 are used. A sample is prepared by sealing a drop (approx 80 μL) of the suspension between two microscope cover slips with a 1mm spacer and Vaseline to prevent leakage. Images and videos are taken using the CCD camera as indicated in Fig. 2. It is found that one or more particles are trapped in the high intensity region of the crescent beam. The particles are trapped in all three directions and can be held at a position well away from the glass/water interface.

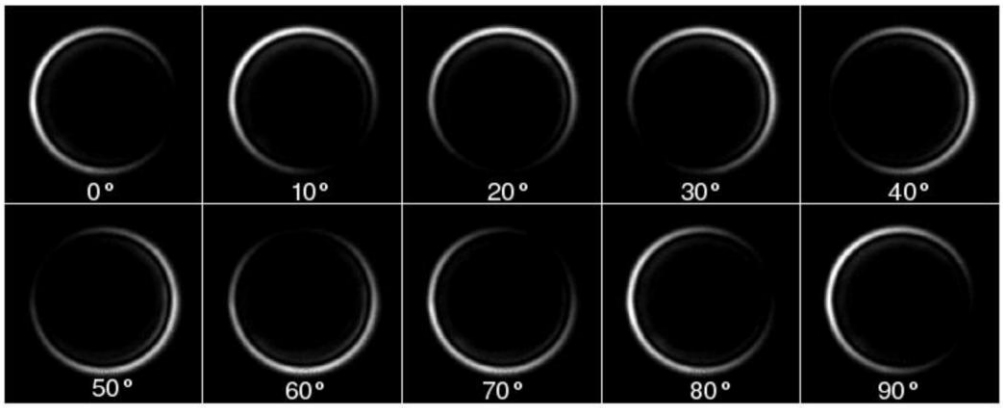


Fig. 3. Intensity profiles at the FIP (11.54 cm beyond $L_1$) as the fast-axis of the half wave-plate is rotated through 90°. Media 1 shows the rotation of the profile that occurs when the half wave-plate is rotated.

Figure 4 shows a sequence of overlayed images of position of a 5.3 μm polystyrene particle trapped in the crescent trap as the wave-plate is rotated at 0.19 Hz and the crescent beam rotates at 0.76 Hz. The images span a 90° rotation of the half wave-plate. This observation clearly demonstrates circular motion of the particle according to the orientation of the wave-plate. Media 2 shows the particle in continuous circulation. The sense of motion is easy to control by reversing the rotation of the wave-plate, see Media 2. Of course, static control of the angular position on the ring is easy to achieve by setting a particular angle of the half wave-plate.

The circulation behaviour of a group of four trapped 5.2 μm melamine-formaledehyde particles is also examined, and Fig. 5(a) shows a sequence of images as the wave-plate is rotated by just over 90°. The relative positions of the particle group and the crescent beam are indicated in the figure. The position of the centre of the trapping beam, which is also the centre of rotation of the particles, is shown. This lies very close to the centre of one of the particles as indicated. Media 3 shows the continuous rotation of the particle group.

#136055 - $15.00 USD Received 4 Oct 2010; revised 12 Nov 2010; accepted 13 Nov 2010; published 13 Dec 2010

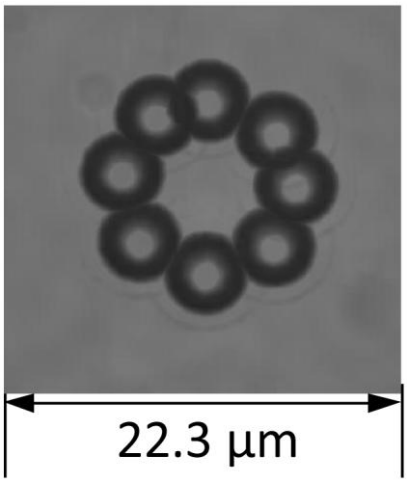


Fig. 4. Selection of overlayed frames from the continuous circular motion of 5.3µm polystyrene particles around a 35µm circumference conical trap rotating at 0.8Hz. Media 2 shows the continuous motion of a single polystyrene particle of 5.3 micron diameter moving both clockwise and anti-clockwise with power of 87 mW and rotation rate of 0.2 Hz.

Figure 5(b) shows the trapping and circulation of a white blood cell. These cells are roughly spherical in shape with a diameter of 8 µm and are suspended in a phosphate buffer saline solution. As before, the cells can be moved on a circle by varying the angle of the incident linear polarisation. Media 4 shows the continuous rotation of the white blood cell.

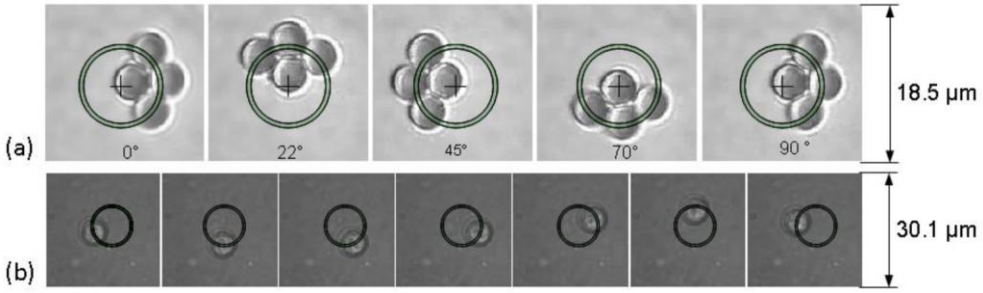


Fig. 5. (a) Optically driven anti-clockwise rotation of a cluster of four 5.3 µm melamine formaldehyde particles. The position of the crescent beam relative to the particles is indicated. Media 3 shows rotation of the 4 melamine formaledehyde particles on the ring with power of 90 mW and rotation rate of 0.22 Hz (b) Circular motion of an 8 µm in diameter white blood cell. Media 4 shows a single white blood cell moving around the circle with 60 mW power and rotation rate of 0.125 Hz.

## 5. Characterisation of the optical trap

We investigated the strength of the optical trap by measuring the maximum radial translation and circulation speeds of 5.3 µm polystyrene particles as a function of optical power in the trapping plane. Firstly, the particle is held in a non-rotating trap and the sample cell is translated along the line joining zero and maximum intensity to exert a viscous drag force pointing radially outwards. Secondly, the maximum circulation frequency for a given power is determined by increasing the rotational frequency of the wave-plate until the trapped particle is lost. This maximum circulation frequency of the particle in the trap enables the determination of the escape velocity ($v_e$) for this circular motion. The maximum trapping forces in the tangential and radial directions can then be calculated using the Stokes equation:

#136055 - $15.00 USD Received 4 Oct 2010; revised 12 Nov 2010; accepted 13 Nov 2010; published 13 Dec 2010

$$F_{opt} = 6\pi R_p \eta v_e \quad (2)$$

where Rp is the radius of the spherical particle and η is the viscosity of water. The results are plotted in Fig. 6; the maximum speed and force vary linearly with optical power. It can be seen that at 100 mW the maximum radial speed is 42 μm $s^{-1}$ and the corresponding trapping force in ~1.8 pN. The power variation of the maximum stable circulation speed and tangential force were also measured and are shown in Fig. 6. As before the maximum force is linearly related to the optical power. In this case for 100 mW the maximum circulation speed is 19 μm $s^{-1}$ and the tangential force is only ~0.8 pN. The tangential force is smaller than the radial force since the gradient of the electric field is smaller in the tangential direction for the crescent beam.

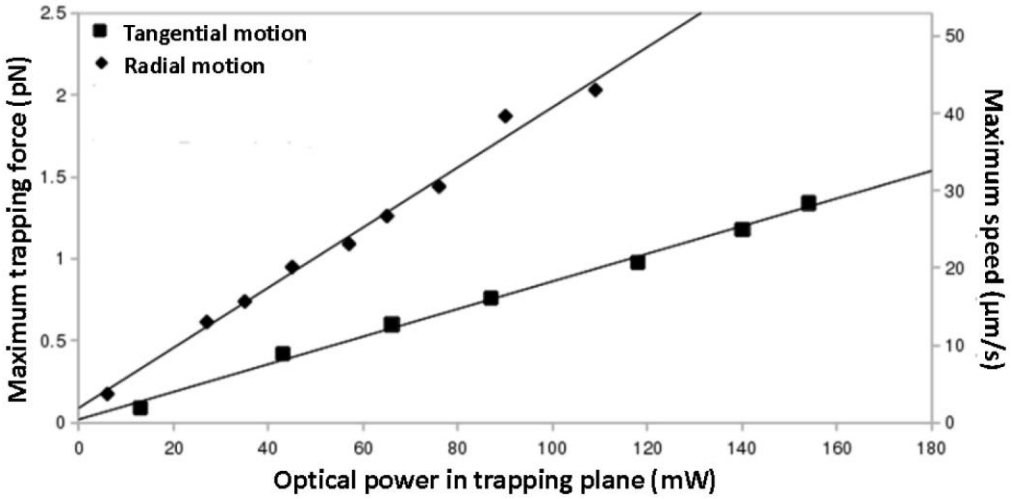


Fig. 6. Dependence of the maximum trapping force and speed versus optical power for the crescent-shaped beam for circular and radial motions.

A numerical simulation of the conical ring trap was performed using the geometric ray optics method described in [6, 26,27]. Briefly, the force acting on a sphere in a beam of light is found by summing up the differential force imparted by each ray over the illuminated area of the sphere for both the scattering and gradient forces. The dimensionless variable Q in Eq. (3) describes the trapping force in terms of the incident momentum for a given power P and the refractive index ratio n of the particle and suspension fluid.

$$F_{opt} = Q\frac{nP}{c} \quad (3)$$

Figure 7(a) shows the variation of the *Q* value as a 5.3 μm radius polystyrene particle is translated from the centre of the crescent beam through the region of maximum intensity. The equilibrium position ($r_{eq}$ = 5.18 μm) is slightly displaced from the position of maximum intensity due to the interaction of the sphere with the weaker inner ring. The *Q* value rises to about 0.006 at $r$ = 7.5 μm. This can be compared with the value of 0.005 obtained from the measured maximum trapping force for radial motion (Fig. 6). Figure 7(b) shows the variation of *Q* as the particle is moved tangentially around ring at the equilibrium radial position $r_{eq}$. As expected the tangential trapping force varies sinusoidally around the ring. It is zero at the positions of minimum ($\theta = \pi$) and maximum ($\theta = 2\pi$) intensity. The simulations show that the maximum radial trapping force is about four times larger than the maximum tangential trapping force, whereas in the experiment the ratio of these forces is about two. In deriving the tangential force from the escape velocity, we used the Stokes equation with $v_e$ equal to the maximum measured tangential speed. Clearly for circular motion of a spherical particle this

#136055 - $15.00 USD Received 4 Oct 2010; revised 12 Nov 2010; accepted 13 Nov 2010; published 13 Dec 2010

only gives an approximate estimate, particularly for our case where the diameter of the particle orbit is only twice the particle diameter. This may account for the apparent discrepency between the measured and calculated

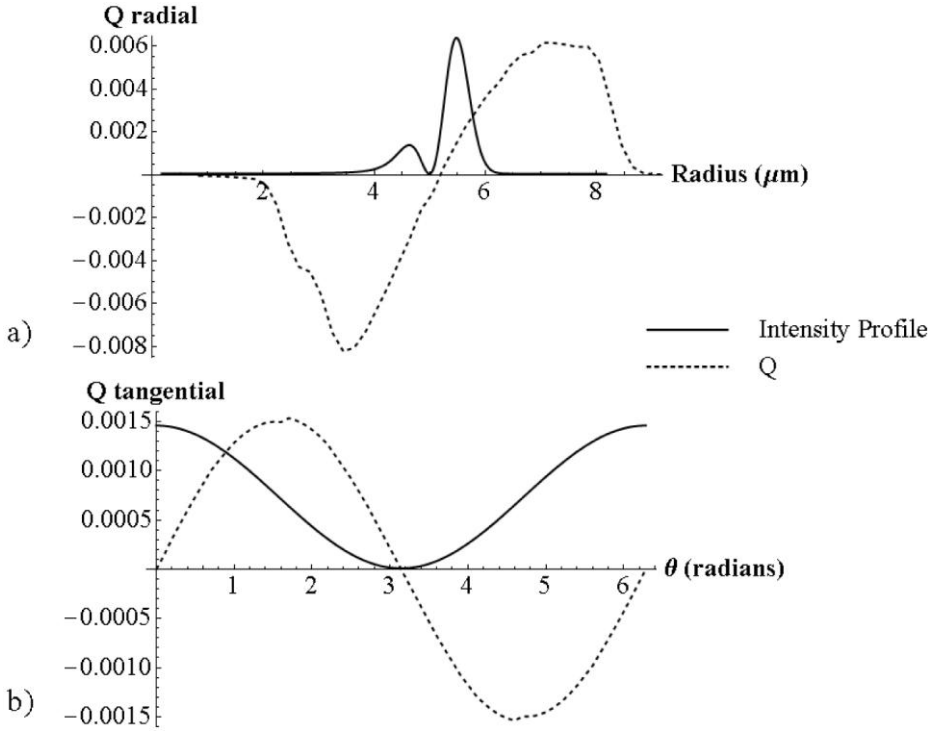


Fig. 7. Simulation of the radial and tangential trapping forces, in terms of the variable $Q$ (dashed), for 5.3 μm radius polystyrene particle in water and using the intensity profile (solid) in the focal plane of the microscope objective. (a) Variation of $Q$ as the particle is translated from the centre of the crescent beam through the region of maximum intensity. (b) Variation of $Q$ around the crescent beam at the equilibrium radial position $r_{eq}$ = 5.18 μm.

## 6. Conclusions

In conclusion, the linearly polarised case of internal conical diffraction produces a crescent-shaped beam whose intensity and polarisation vary in a unique way. Rotation of the plane of the linearly polarised light moves the intensity maximum around the ring. This unusual behaviour in an optical beam has been used in an optical trap where the polarisation is used to control the angular position. The trap is simple to construct and easy to adjust suggesting that it will find application in the manipulation of small particles and driving micro-machines. The relatively small values of the trapping forces observed here is due to the fact that the trapped particle only intercepts a fraction of the trapping beam and the microscope system is quite basic. The strength of the trap in the tangential direction can be increased by placing a polariser after the crystal with its transmission axis set parallel to the input polarisation. The azimuthal intensity distribution is then given by $\cos^4(\theta/2)$ and the intensity gradient is correspondingly higher. The radius of the crescent-shaped trap can be varied by introducing a zoom lens into the system to dynamically adjust the diameter $R_0$ in the FIP, and thus the ring diameter in the trapping plane.


## Acknowledgements

This work was supported by Science Foundation Ireland under its PI programme, grant number 07/IN.1/I1862.


#136055 - $15.00 USD Received 4 Oct 2010; revised 12 Nov 2010; accepted 13 Nov 2010; published 13 Dec 2010